Enhanced bacterial killing by vancomycin in staphylococcal biofilms disrupted by novel, DMMA-modified carbon dots depends on EPS production

Wu, Yanyan; van der Mei, Henny C.; Busscher, Henk J.; Ren, Yijin

Published in:
COLLOIDS AND SURFACES B-BIOINTERFACES

DOI:
10.1016/j.colsurfb.2020.111114

Colloids and Surfaces B: Biointerfaces 193 (2020) 111114

Contents lists available at ScienceDirect

Colloids and Surfaces B: Biointerfaces

journal homepage: www.elsevier.com/locate/colsurfb

Enhanced bacterial killing by vancomycin in staphylococcal biofilms disrupted by novel, DMMA-modified carbon dots depends on EPS production

Yanyan Wu[a], Henny C. van der Mei[b,*], Henk J. Busscher[b,*], Yijin Ren[a]

[a] University of Groningen and University Medical Center of Groningen Department of Orthodontics, Hanzeplein 1, 9700 RB Groningen, the Netherlands
[b] University of Groningen and University Medical Center Groningen Department of Biomedical Engineering, Antonius Deusinglaan 1, 9713 AV Groningen, the Netherlands

ARTICLE INFO

Keywords:
Infection
Penetration
Disruptant
Dispersant
Accumulation
Antibiotic treatment

ABSTRACT

Alternatives for less and less effective antibiotic treatment of bacterial infections, are amongst others based on nanotechnological innovations, like carbon-dots. However, with a focus on chemistry, important characteristics of bacterial strains, like (in-)ability to produce extracellular-polymeric-substances (EPS) are often neglected. EPS is the glue that certain bacterial strains produce to keep a biofilm together. Here we report on synthesis of novel, pH-responsive, 2,3-dimethylmaleic-anhydride modified carbon-dots (C_{DMMA}-dots). C_{DMMA}-dots, like unmodified C-dots without DMMA, were little bactericidal. However, C_{DMMA}-dots reduced volumetric-bacterial-density within the acidic-environment of a biofilm for a non-EPS-producing *Staphylococcus epidermidis* strain, indicative for a more open structure. Such a structural disruption was not observed for an EPS-producing strain. Disrupted biofilms of the non-EPS-producing strain pre-exposed to C_{DMMA}-dots at pH 5.0, were more amenable to vancomycin penetration and killing of their inhabitants than biofilms of EPS-producing-staphylococci. Herewith, we describe a new role of carbon-dots as synthetic disruptants of biofilm structure. It is a partial success story, identifying the challenge of making carbon-dots that act as a universal disruptant for biofilms of strains with different microbiological characteristics, most notably the ability to produce or not-produce EPS. Such carbon-dots, will enable more effective clinical treatment of bacterial infections combined with current antibiotics.

1. Introduction

Persistent bacterial infections remain a major threat to public health [1], especially since available antibiotics are becoming less and less effective due to the increasing occurrence of multi-drug resistant strains and the biofilm mode of growth in which the majority of bacterial infections presents themselves [2]. Biofilms are surface-attached and surface-adapted, densely populated communities of bacteria encapsulated in a matrix of self-generated, Extracellular Polymeric Substances (EPS) [2–4]. Notwithstanding the presence of bacteria and EPS, biofilms are comprised for more than 80 wt% of water, possibly with dissolved EPS [4]. The EPS matrix is generated once bacteria sense that they are surface-attached and protects adhering bacteria against environmental attacks, such as by antibiotics [2]. Bacteria in a biofilm mode of growth can be up to 1000-fold more resistant to antibiotics than planktonic bacteria free in suspension, which adds to the intrinsic resistance a bacterial strain may have against an antibiotic [5]. The quest for direly needed, new infection-control strategies should therefore not only focus on new antimicrobials with the ability to kill planktonic bacteria in suspension, but also on strategies that allow antimicrobials to penetrate into infectious biofilms [6–8]. Without deep penetration into a biofilm, and associated bacterial killing across the entire depth of a biofilm, infections will be re-current [1].

Antimicrobial nanoparticles and nanotechnology-based encapsulated antimicrobials [9], are generally considered promising alternatives for infection-control, but most studies focus on chemistry and neglect important characteristics of the bacterial strains used for evaluation, like the (in-)ability to produce EPS. Neglect of bacterial strain characteristics leaves a large step toward human clinical translation and even toward animal experiments that become more and more strictly regulated [10]. This neglect will eventually form an impediment to clinical translation and use.

Carbon dots form an interesting class of nanoparticles that can be prepared at low costs and generally possess good biocompatibility [11,12]. Carbon dots can be surface-modified for application in bioanalysis, bioimaging, delivery of chemotherapeutics for tumor treatment

* Corresponding authors.
E-mail addresses: h.c.van.der.mei@umcg.nl (H.C. van der Mei), h.j.busscher@umcg.nl (H.J. Busscher).

https://doi.org/10.1016/j.colsurfb.2020.111114
Received 18 March 2020; Received in revised form 4 May 2020; Accepted 5 May 2020
Available online 12 May 2020

[13–18] and recently also for infection-control [19–23]. Carbon dots can be made from various sources [24,25] with an impact on their antimicrobial properties. Carbon dots synthesized from graphene have the ability to catalyze the decomposition of H_2O_2 to yield an alkaline environment, with antibacterial activity against Gram-negative *Escherichia coli* and Gram-positive *Staphylococcus aureus* [21]. Hydrothermal carbonization of vitamin C [26] or bacteria (*E. coli* and *S. aureus*) [27] yielded negatively-charged carbon dots. Vitamin C-derived carbon dots possessed anti-adhesion and antibacterial properties [26], while bacteria-derived carbon dots selectively targeted dead bacteria to differentiate them from live ones [27]. Carbon dots obtained through hydrothermal carbonization of *Lactobacillus plantarum* inhibited *E. coli* growth and were non-cytotoxic [22]. Positively-charged carbon dots, prepared from glycerol and 3-[2-(2 aminoethylamino)ethylamino] propyl-trimethoxysilane and conjugated with a quaternary ammonium compound, displayed antibacterial activity against *E. coli* and *S. aureus* [28].

Rather than using carbon dots as a stand-alone antimicrobial to attack infectious biofilms, we believe that their use in combination with clinically applied antibiotics may form an attractive pathway to pave the way for the clinical translation of carbon dots as a new, stand-alone antimicrobial. Here we report on the synthesis of 2,3-dimethylmaleic anhydride (DMMA) modified, pH-responsive carbon dots (C_{DMMA}-dots) for therapeutic use together with a clinically applied antibiotic (i.e. eradication an existing biofilm as opposed to prophylactically inhibiting biofilm formation and growth). Carbon dots were prepared through heating of citric acid as a carbon source and a branched polyethyleneimine as a passivating agent. Thus prepared C-dots without DMMA were conjugated with DMMA. C_{DMMA}-dots were subsequently studied in comparison with C-dots without DMMA with respect to their ability to eradicate existing *Staphylococcus epidermidis* biofilms in combination with vancomycin. *S. epidermidis* is a commensal of the skin [29], and therewith frequently gaining access to the human body during invasive surgery or trauma to form an infectious biofilm [30]. Considering the importance of the EPS matrix in the penetration and killing of biofilm inhabitants by antimicrobials, a known non-EPS and EPS producing *S. epidermidis* strain were evaluated in this study. Previous studies have identified the (in)ability of these strain to produce EPS using calcofluor white staining of biofilms followed by fluorescence microscopy [31], PCR [32] and Congo red agar plating [33].

2. Results and discussion

In this work, we selected hydrothermally prepared C-dots using citric acid as a carbon source and polyethyleneimine as a surface passivating agent [16,18]. Thus prepared C-dots were selected because they have been described to inherently display positively-charged amine groups, strong fluorescence and high photostability [16,18]. To provide C-dots with pH-responsiveness, these amine-groups in the C-dots were conjugated with DMMA to produce C_{DMMA}-dots. Successful conjugation of DMMA can be inferred from a comparison of the NMR spectra of C-dots without DMMA and C_{DMMA}-dots. ^{1}H NMR spectra of C_{DMMA}-dots showed peaks around 1.85 and 1.72 ppm that were absent in the corresponding spectrum of C-dots (Fig. 1a), indicative of methyl-groups (-C(CH_3)=C(CH_3)-). In line, ^{13}C NMR spectra of C_{DMMA}-dots demonstrated new peaks correlating with alkenes at 137.7 ppm and 132.9 ppm (Fig. 1b) that were absent in spectra of C-dots without DMMA. New peaks at 179.3 ppm and 173.5 ppm corresponded to carboxylic acid and amide groups in C_{DMMA}-dots. New peaks at 8.0 and 15.5 ppm can be assigned to methyl groups. Presence of DMMA could furthermore be inferred from UV–vis spectroscopy, demonstrating a clear peak around 230 nm (Fig. 1c) in C_{DMMA}-dots that is absent in C-dots without DMMA [16,18].

Fluorescence emission spectra (Fig. S1) of C-dots without DMMA and C_{DMMA}-dots were measured for carbon dot suspensions in phosphate buffer at pH 5.0 and 7.4 and both demonstrated emission peaks at similar wavelengths upon excitation at pH 5.0 and pH 7.4. However, emission peaks of C_{DMMA}-dots occurred at slightly lower wavelengths than of C-dots without DMMA. The quantum yield of the carbon dots was measured relative to quinine sulfate as a standard and found to be 9.4% and 11.1% for C-dots without DMMA in phosphate buffer at pH 7.4 and 5.0, respectively. Quantum yields were slightly less for C_{DMMA}-dots (5.0% at pH 7.4 and 8.0% at pH 5.0) (Fig. 2). The quantum yield of our carbon dots was similar to previously reported quantum yields in buffer for carbon dots [34].

Both C-dots without DMMA and C_{DMMA}-dots possessed spherical shapes (Fig. 3a) with average hydrodynamic diameters over three separately prepared batches of 6.0 ± 0.4 nm and 14.0 ± 0.9 nm for C-dots and C_{DMMA}-dots, respectively (note that ± denotes the standard deviation over the mode of three distributions measured over separately prepared batches of carbon dots). Zeta potentials of C-dots without DMMA at pH 7.4 (Fig. 3b) were stable over time and slightly positive due to the surface exposure of amine groups inherent to their preparation. Zeta potentials of the C-dots without DMMA became more positive at pH 5.0 (+17.8 mV) due to the pH-responsiveness of the amine groups without measurable delay and were stable in time. Zeta potentials of C_{DMMA}-dots were also stable over time at pH 7.4 (Fig. 3c), but opposite to C-dots without DMMA, slightly negative due to negatively charged dimethylmaleic acid (carboxyl-) groups. However, C_{DMMA}-dots at pH 5.0 showed a time-dependent increase of their zeta potentials from about +0.9 mV to about +15 mV within 1 h due to generation of cationic amino groups after cleavage of amide linkages.

Carbon dot interaction with *S. epidermidis* ATCC 12228 (a non-EPS-producing strain) [31–33] and *S. epidermidis* ATCC 35984 (an EPS-producing strain) [31–33] was first studied by measuring zeta potentials. To this end, planktonic staphylococci were exposed to increasing concentrations of carbon dots at the physiological pH of 7.4 and at pH 5.0, as prevailing in many infectious biofilms [35,36]. Occurrence of less negative and positive staphylococcal zeta potentials after exposure to carbon dots may influence their ability to attach to each other and aggregate, as being controlled by electrostatic double-layer interactions acting in concert with hydrophobic interactions [37]. In absence of carbon dots, both *S. epidermidis* ATCC 12228 and ATCC 35984 possessed highly negative zeta potentials of −28.9/−26.9 mV and −25.5/−20.3 mV (at pH 7.4/5.0), respectively (Fig. 3d and e). Zeta potentials of both strains became positive after exposure to C-dots without DMMA irrespective of pH, indicating binding of the positively-charged C-dots without DMMA to the negatively-charged bacterial surfaces. After staphylococcal exposure to C_{DMMA}-dots at pH 7.4, however, both strains only became less negatively-charged without a charge reversal, while exposure at pH 5.0 yielded positive zeta potentials, comparable with zeta potentials after exposure to C-dots without DMMA. Summarizing, exposure of staphylococci to either type of carbon dots, reduced the absolute value of their zeta potentials, whether positive or negative. Therewith electrostatic double-layer repulsion between equally-charged staphylococci has decreased and their tendency to aggregate has increased.

Since biofilms are comprised predominantly of water [4], the ability of staphylococci to attach to surfaces prior to and after exposure to carbon dots was therefore further assessed by measuring their partitioning from an aqueous phase toward hydrophobic hexadecane droplets [38,39]. Hexadecane droplets suspended in phosphate buffers are known to be hydrophobic and negatively charged [40] and partitioning from an aqueous phase to the hexadecane phase depends on an interplay of hydrophobic and electrostatic double-layer attraction [41]. Removal from the aqueous phase of staphylococci prior to exposure to carbon dots was extremely low at all pH values (Fig. 3f and g).

Exposure to C-dots without DMMA increased the initial removal rates of both staphylococcal strains from the aqueous phase to the hexadecane phase regardless of pH (see also Fig. 3f and g), therewith indicating increased involvement of pH-independent hydrophobic attraction driving the staphylococci toward the hexadecane phase.

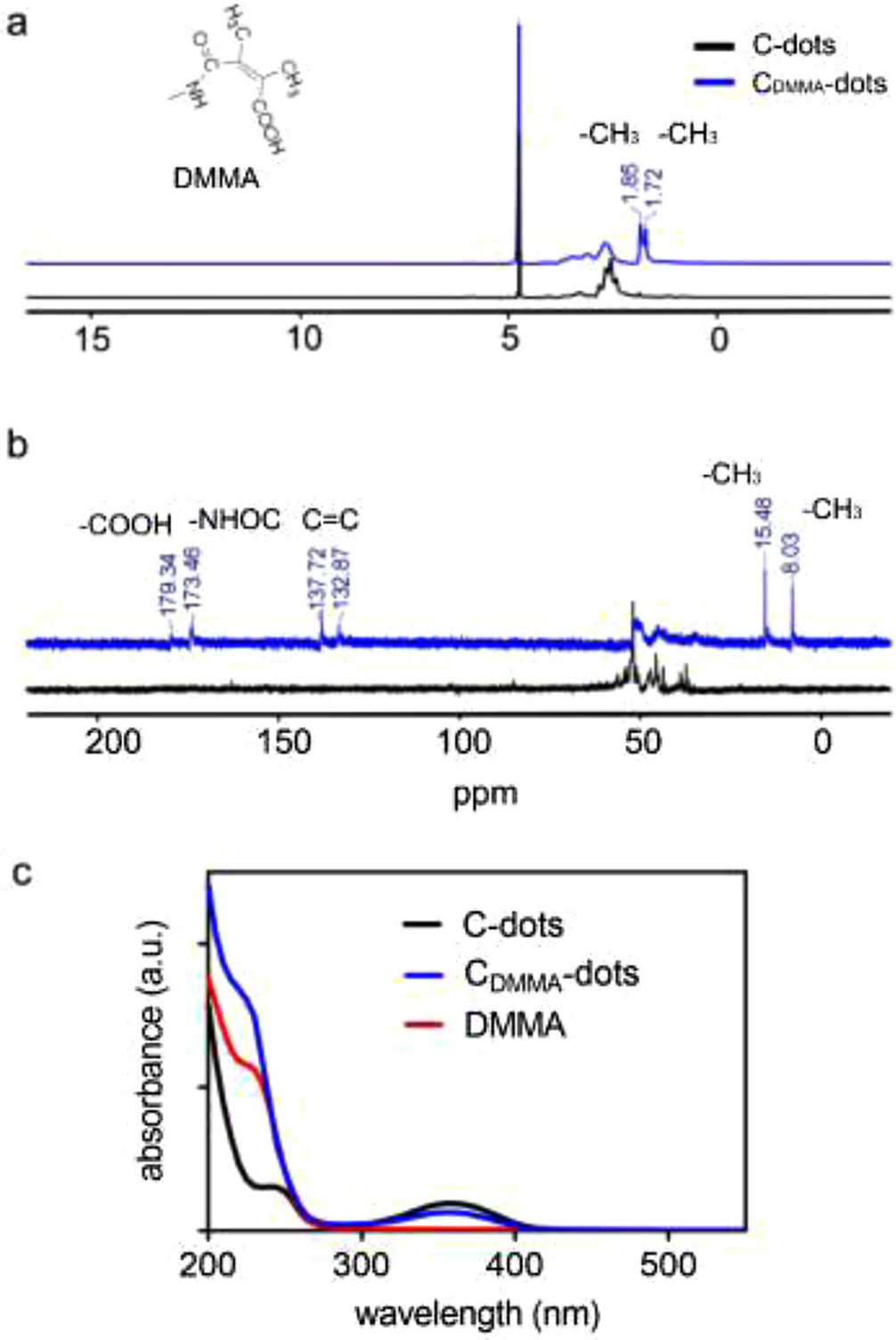

Fig. 1. (a) ^{1}H NMR spectra of C-dots without DMMA and C_{DMMA}-dots in D_2O.
(b) ^{13}C NMR spectra of C-dots without DMMA and C_{DMMA}-dots in D_2O water.
c) UV–vis absorption spectra of C-dots without DMMA, C_{DMMA}-dots and DMMA in water.

However, removal from the aqueous phase of staphylococci exposed to C_{DMMA}-dots was pH-dependent. Moreover, below pH 6, removal of staphylococci with attached C_{DMMA}-dots exceeded removal of bacteria with attached C-dots. Considering that exposure of staphylococci to either type of carbon dots yields similarly positive zeta potentials, it can be concluded that the higher removal from an aqueous phase of staphylococci exposed to C_{DMMA}-dots at low pH (< 6.0) is due to stronger hydrophobic attraction than exerted by staphylococci exposed to C-dots without DMMA.

Bactericidal activity of the C_{DMMA}-dots against planktonic *S. epidermidis* was derived from their MBC (minimal bactericidal concentration; see Table 1) and compared with the antibacterial activity of C-dots without DMMA and DMMA in solution. DMMA possessed no noteworthy bactericidal activity, regardless of pH. The positively charged C-

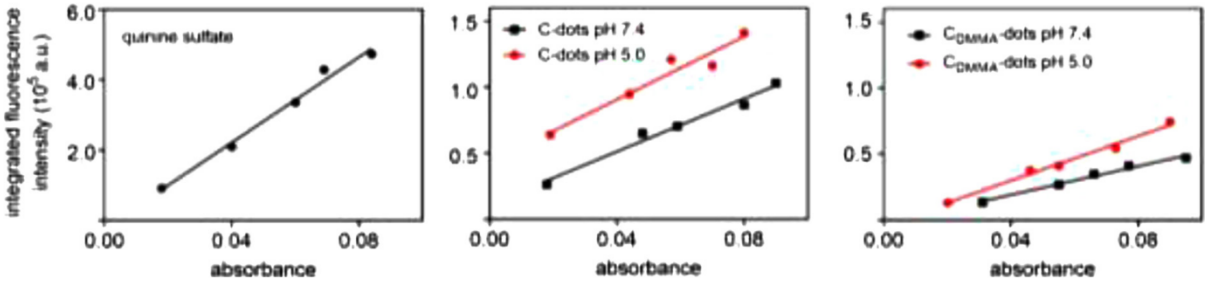

Fig. 2. Integrated fluorescence intensity as a function of absorbance of C-dots without DMMA and C_{DMMA}-dots at pH 5.0 and 7.4. The ratio of absorption to emission was derived by linear interpolation (drawn lines), while calculating the quantum yield from the slopes relative to the slope for quinine sulfate with a known quantum yield (54%).

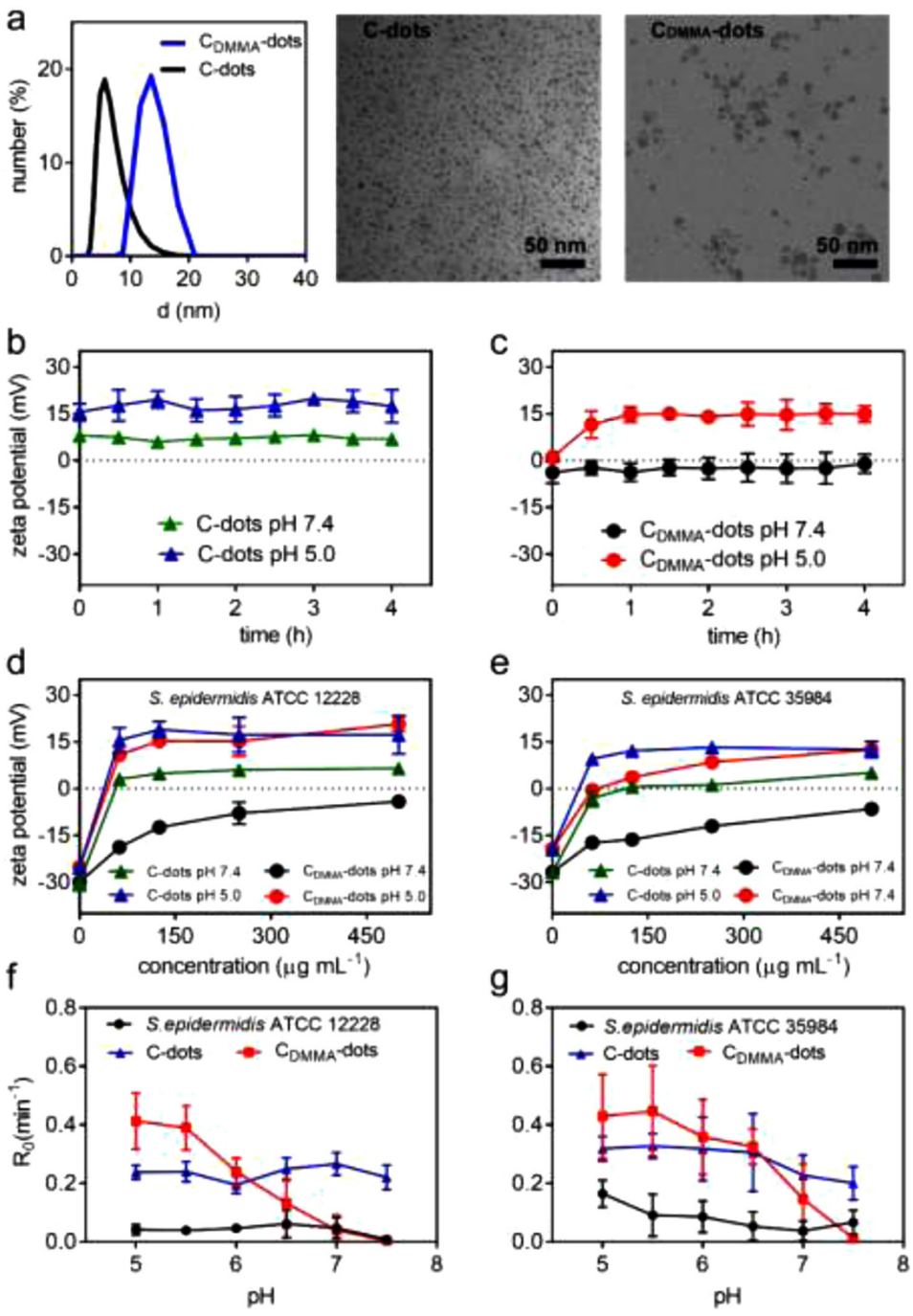

Fig. 3. (a) Hydrodynamic diameters of C-dots without DMMA and C_{DMMA}-dots measured in 10 mM potassium phosphate buffer (pH 7.4) using Dynamic Light Scattering, together with TEM images of both types of carbon dots.
(b) Zeta potentials of C-dots without DMMA as a function of time in 10 mM potassium phosphate buffer at pH 7.4 and pH 5.0.
(c) Same as (b), but now for C_{DMMA}-dots.
(d) Zeta potentials of *S. epidermidis* ATCC 12228 after 30 min exposure to C-dots without DMMA or C_{DMMA}-dots in 10 mM potassium phosphate buffer as a function of the concentration of carbon dots.
(e) Same as panel (d), but now for *S. epidermidis* ATCC 35984.
(f) Initial microbial removal rates R_0 of *S. epidermidis* ATCC 12228 in two-phase partitioning prior to and after exposure to carbon dots as a function of pH in 10 mM potassium phosphate buffer.
(g) Same as panel (f), but now for *S. epidermidis* ATCC 35984.
All data are expressed as means ± standard deviations (SD) over triplicate experiments with separately prepared carbon dots and different staphylococcal cultures.

Table 1
Minimal bactericidal concentrations (MBC) of non-EPS producing *S. epidermidis* ATCC 12228 and EPS-producing *S. epidermidis* ATCC 35984 to DMMA in solution, C-dots without DMMA and C_{DMMA}-dots, measured in 15% TSB at pH 7.4 and 5.0. Experiments were conducted in 15% TSB rather than in full medium, because carbon dot suspensions were instable in full medium.

	pH 7.4			pH 5.0		
Strain	DMMA (μg mL^{-1})	C-dots without DMMA (μg mL^{-1})	C_{DMMA}-dots (μg mL^{-1})	DMMA (μg mL^{-1})	C-dots Without DMMA (μg mL^{-1})	C_{DMMA}-dots (μg mL^{-1})
S. epidermidis ATCC 12228	1000	15.6	> 1000	500	7.81	62.5
S. epidermidis ATCC 35984	1000	62.5	> 1000	500	31.25	250

dots without DMMA possessed a small bactericidal activity at relatively high MBCs against both planktonic *S. epidermidis* strains at pH 7.4 and 5.0, while C_{DMMA}-dots also killed bacteria only at a relatively high MBC, especially at pH 7.4.

Subsequently, *S. epidermidis* biofilms were exposed to either type of carbon dots or DMMA in solution to demonstrate their ability to penetrate and accumulate in the biofilms at different pH. Due to the blue-fluorescence of citric acid/polyethyleneimine derived C-dots without DMMA and C_{DMMA}-dots [16,18], their presence in biofilms could be easily distinguished from live, green-fluorescent (SYTO9 stained), and dead, red-fluorescent (propidium iodide stained) staphylococci using CLSM imaging. Biofilms of non-EPS producing *S. epidermidis* ATCC 12228 and EPS producing *S. epidermidis* ATCC 35984had similar thicknesses of 40 ± 5 μm and 42 ± 3 μm, respectively regardless of the pH of the buffer it was immersed in (± standard deviation over triplicate experiments). *S. epidermidis* ATCC 12228 biofilms remained fully intact upon exposure to C-dots without DMMA both at pH 7.4 (Fig. 4a) and pH 5.0 (Fig. 4b), yielding few, scattered dead bacteria in the biofilm particularly at pH 5.0 and in line with the pH-dependence of their relatively high MBC (see Table 1). However, C-dots without DMMA penetrated and accumulated more in *S. epidermidis* ATCC 12228 biofilms at pH 5.0 than at pH 7.4 (compare Fig. 4a and b). Exposure to C_{DMMA}-dots at pH 7.4 did not lead to observable penetration and accumulation in *S. epidermidis* ATCC 12228 (Fig. 4a), but at pH 5.0 uniquely created holes in biofilms of non-EPS producing *S. epidermidis* ATCC 12228 (Fig. 4b). Such holes were not created by only DMMA in solution (Fig. S2a and S2b) nor in biofilms of EPS-producing *S. epidermidis* ATCC 35984 (Fig. 4c and d), regardless of pH.

Disruption of non-EPS producing *S. epidermidis* ATCC 12228 biofilms at pH 5.0 upon exposure to C_{DMMA}-dots can be explained by stronger hydrophobic attraction combined with lower electrostatic double-layer repulsion between biofilm inhabitants as compared with pH 7.4 and upon exposure to C-dots without DMMA. Exposure of biofilms formed by EPS-producing *S. epidermidis* ATCC 35984 upon exposure to C_{DMMA}-dots did not create any holes in the biofilm, likely due to a higher visco-elasticity of the EPS-laden biofilm matrix produced [42]. This visco-elastic, mechanical resistance hampers movement of individual staphylococci toward each other, impeding aggregation and therewith no hole formation.

Next, biovolumes and volumetric bacterial densities were derived from the CLSM images, using ImageJ and COMSTAT [43]. Biovolumes after 4 h exposure to buffer or either type of carbon dot suspensions were for the major part composed of green-fluorescent pixels, in line with the few scattered red-fluorescent, dead staphylococci observed in biofilm images (Fig. 4). Only exposure of non-EPS producing *S. epidermidis* ATCC 12228 to C_{DMMA}-dots at pH 5.0 caused a significant decrease in biovolume (Fig. 5a), that was time-dependent (Fig. S3). Neither exposure to DMMA in solution (Fig. S2c) nor C-dots without DMMA caused a decrease in biovolume. For EPS producing *S. epidermidis* ATCC 35984 no significant reductions in biovolumes were observed for neither type of carbon dots, regardless of pH (Fig. 5c and Fig S3 for kinetics). The observation of holes in *S. epidermidis* ATCC 12228 biofilms after exposure to C_{DMMA}-dots at pH 5.0 due to bacterial aggregation resulting from increased hydrophobic attraction and decreased electrostatic double-layer repulsion between bacteria, suggests altered volumetric bacterial densities in the biofilms (i.e. the number of live and dead bacteria (see Table S1) per unit volume in a biofilm). In line with this suggestion, a significant decrease in volumetric bacterial density was only observed upon 4 h exposure of *S. epidermidis* ATCC 12228 to C_{DMMA}-dots at pH 5.0 (Fig. 5b), but not for biofilms of *S. epidermidis* ATCC 35984 (Fig. 5d). Interestingly, a significant decrease in volumetric bacterial density commenced already after 1 h exposure to C_{DMMA}-dot suspensions, while a significant biovolume decrease set in only after 4 h (see Fig. S3). Thus, changes in biovolume and volumetric bacterial densities are independent processes. Decreases in volumetric bacterial density are indicative of a more open, disrupted structure of the biofilm and may be the on-set of reduction in biovolume that is indicative of biofilm dispersal, i.e. bacterial detachment from a biofilm. In this perspective, biofilm disruption can be considered as a precursor of biofilm dispersal. Known biofilm dispersants can be of bacterial or synthetic origin and are generally considered as a possible new infection-control strategy since the immune system deals easier with planktonic bacteria than with bacteria in a biofilm mode of growth [5]. Dispersal of infecting biofilms into the blood circulation may also make bacteria more amenable to antibiotic killing [44]. As an advantage above naturally occurring, bacterial dispersants, synthetic dispersants including precursor C_{DMMA}-dot disruptants, are usually more stable [45]. However, at the same time dispersal yields the risk of spreading of infectious bacteria through the body. This risk is absent with a biofilm disruptant.

Since lower volumetric bacterial densities and the accompanying more open structure created by synthetic C_{DMMA}-dot dispersant as described here, can create a more open, less dense biofilms in staphylococcal biofilms of strains that do not produce an extensive EPS matrix might imply better penetration and deeper killing by antibiotics, 24 h old staphylococcal biofilms were first exposed to carbon dot suspensions followed by growth in absence or presence of vancomycin. Pre-exposure to suspensions of C-dots without DMMA did not affect subsequent growth of staphylococci during 24 or 72 h, as compared with pre-exposure to buffer (Fig. 6). Oppositely, compared with pre-exposure to buffer or C-dots without DMMA, pre-exposure to C_{DMMA}-dot suspensions at pH 5.0 yielded significantly better killing of non-EPS producing *S. epidermidis* ATCC 12228 during subsequent growth in presence of 20x MBC vancomycin, especially after 72 h (Fig. 6a and b). This was not the case for biofilms of EPS producing *S. epidermidis* ATCC 35984 (Fig. 6c and d), corresponding with the absence of the formation of holes and decreases in volumetric bacterial densities upon exposure to C_{DMMA}-dot suspensions at pH 5.0.

3. Conclusion

In summary, this study demonstrates that neither DMMA in solution, nor citric acid derived C-dots without DMMA or DMMA modified C_{DMMA}-dots possess any significant bactericidal activity, unlike carbon dots derived from spermine [46], graphene [21], or C60 cage [47]. However, here an entirely new role is identified for non-bactericidal C_{DMMA}-dots as a synthetic biofilm disruptant, affecting the structure of a biofilms of non-EPS producing staphylococci. C_{DMMA}-dots induce

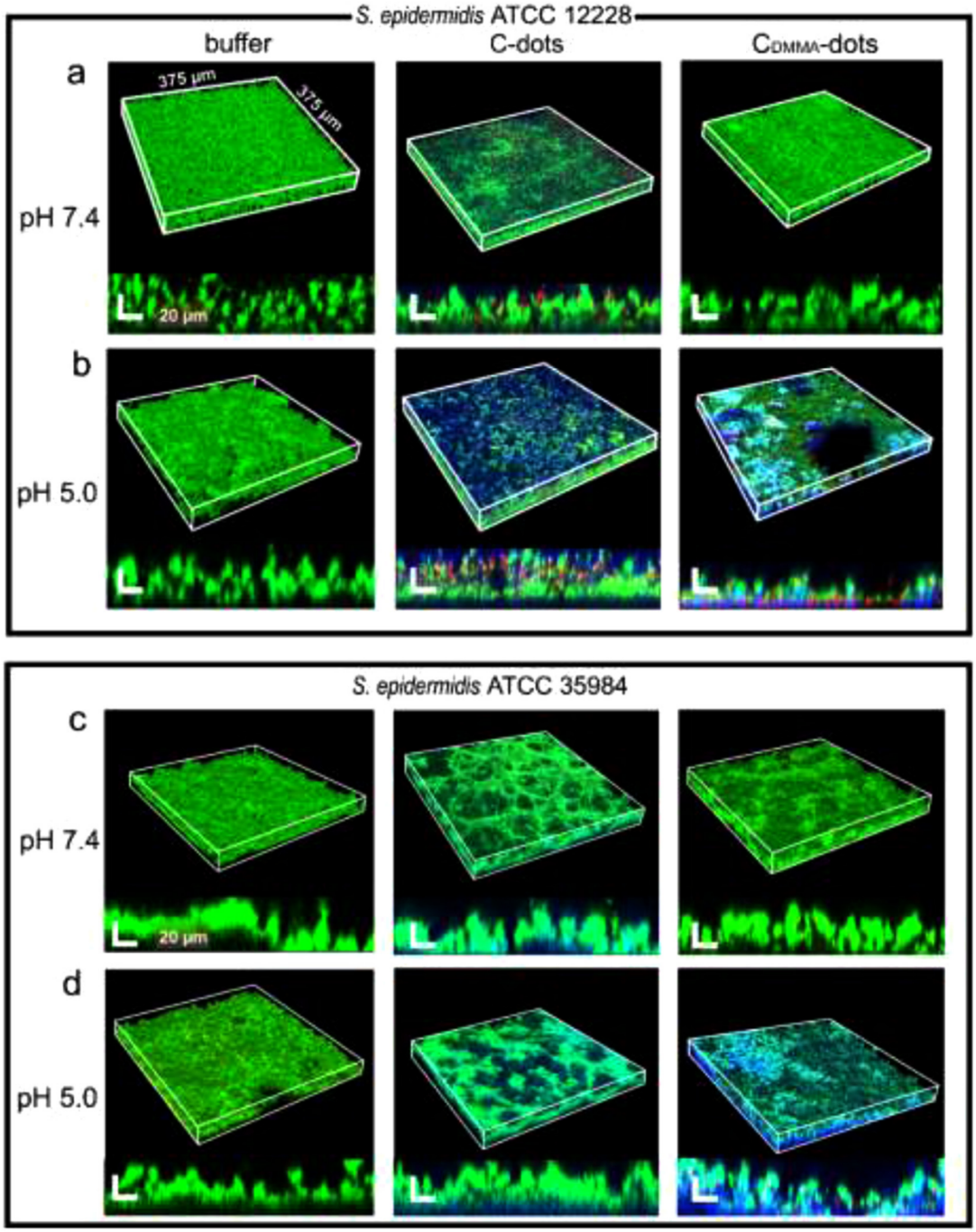

Fig. 4. Penetration and accumulation of C-dots without DMMA and C_{DMMA}-dots in staphylococcal biofilms. Staphylococci were stained with SYTO9 (green-fluorescent) and propidium iodide (red-fluorescent), while citric acid/polyethyleneimine derived carbon dots are blue-fluorescent by themselves [15,17]. Imaging was done using CLSM. (For interpretation of the references to color in this figure legend, the reader is referred to the web version of this article).
(a) Examples of overlayer and cross-sectional images of non-EPS producing *S. epidermidis* ATCC 12228 biofilms after 4 h exposure to buffer, 125 µg mL^{-1} C-dots without DMMA or C_{DMMA}-dots in 10 mM phosphate buffer at pH 7.4. Note the presence of scattered dead staphylococci.
(b) Same as panel (a), now for pH 5.0. Note the presence of scattered dead staphylococci and the creation of holes in the biofilm at pH 5.0.
(c) and (d) Same as examples in panels (a) and (b) respectively, now for EPS producing *S. epidermidis* ATCC 35984.

structural changes in the acidic environment of a biofilm by creating holes and lower volumetric bacterial densities in biofilms. This occurs through increased hydrophobic attraction and reduced electrostatic double-layer repulsion between biofilm inhabitants upon exposure to C_{DMMA}-dot suspensions. Herewith, disruptants create a more open biofilm structure that allows better antibiotic penetration.

Many publications in the literature on new infection-control strategies neglect important microbiological characteristics of bacterial target strains, creating a success story [26,48,49]. We describe a partial success story, showing that exposure of a biofilm of a non-EPS producing staphylococcal strain to C_{DMMA}-dot suspensions makes the biofilm more open to increase the efficacy of a clinically applied antibiotic. Such effects were absent for biofilms of staphylococci that have the ability to produce EPS. Concluding, C_{DMMA}-dots are *promising* as a new infection-control aid with special strength on bacterial strains that do not produce EPS. Future work on the modification of carbon dots to

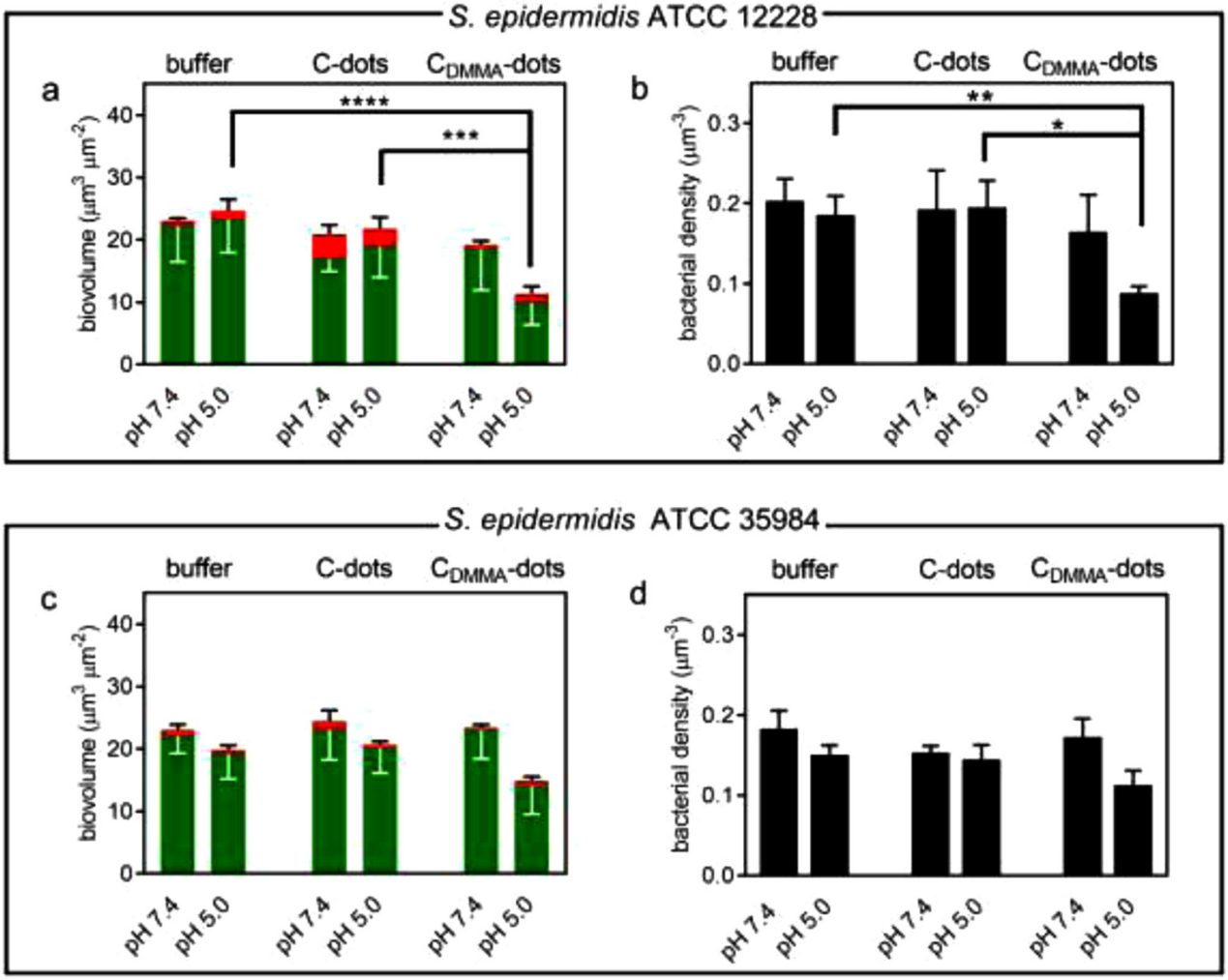

Fig. 5. Disruption of staphylococcal biofilms upon exposure to C- dots without DMMA or C_{DMMA}-dots.
(a) Biovolume of non-EPS producing *S. epidermidis* ATCC 12228 biofilms after 4 h exposure to buffer or suspensions with 125 μg mL^{-1} C-dots without DMMA or C_{DMMA}-dots at pH 7.4 and pH 5.0.
(b) Volumetric bacterial densities of *S. epidermidis* ATCC 12228 biofilms after 4 h exposure to buffer or suspensions with 125 μg mL^{-1} C-dots without DMMA or C_{DMMA}-dots at pH 7.4 and pH 5.0.
(c) Same as panel (a), but now for EPS producing *S. epidermidis* ATCC 35984 biofilms.
(d) Same as panel (b), but now for *S. epidermidis* ATCC 35984 biofilms.
Staphylococci with intact membranes are indicated in green, membrane-damaged bacteria in red. All data are expressed as means ± SD over triplicate experiments with separately prepared nanoparticles and different staphylococcal cultures. *$p < 0.05$ and ****$p < 0.0001$ indicate significant differences with respect to exposure to buffer or C-dot suspensions (one way ANOVA). (For interpretation of the references to color in this figure legend, the reader is referred to the web version of this article).

make them a more general disruptant of infectious biofilms, should focus on strains with known microbiological characteristics, most notably the ability to produce EPS.

4. Methods

4.1. Materials

Branched polyethyleneimine (MW 10,000) was purchased from Alfa Aesar (The Netherlands). Citric acid was purchased from Merck (Germany). 2,3-dimethylmaleic anhydride (DMMA) was purchased from Sigma-Aldrich (The Netherlands). All chemicals were used as received.

4.2. Preparation and characterization of carbon dots

C-dots without DMMA were prepared according to a previously reported method [16]. Briefly, citric acid (0.6 *g*) as a carbon source, branched polyethyleneimine (1.6 *g*, MW 10,000) as a passivating agent and demineralized water (40 mL) were mixed, added into a 100 mL Teflon-lined autoclave and heated at 200 °C for 8 h. In order to remove large dots, the brown solution was centrifuged at 15,800 *g* for 15 min. For further purification, the supernatant was dialyzed against demineralized water (cut-off 14,000 MW) for 3 days, while stirring at room temperature and refreshing the water 3 times a day. C-dots obtained were freeze-dried and stored at 4 °C.

For the preparation of C_{DMMA}-dots, C-dots without DMMA (50 mg) were suspended in demineralized water (5 mL) and pH adjusted to 8.5 using NaOH (0.2 mol L^{-1}). DMMA (350 mg) was gradually added into the C-dot suspension, while stirring and keeping the pH at 8.5 at room temperature for 3 h. The DMMA-modified C-dots were first dialyzed against demineralized water for 1 day to remove the unbound DMMA, refreshing the water every 8 h, after which the C_{DMMA}-dots were freeze-dried.

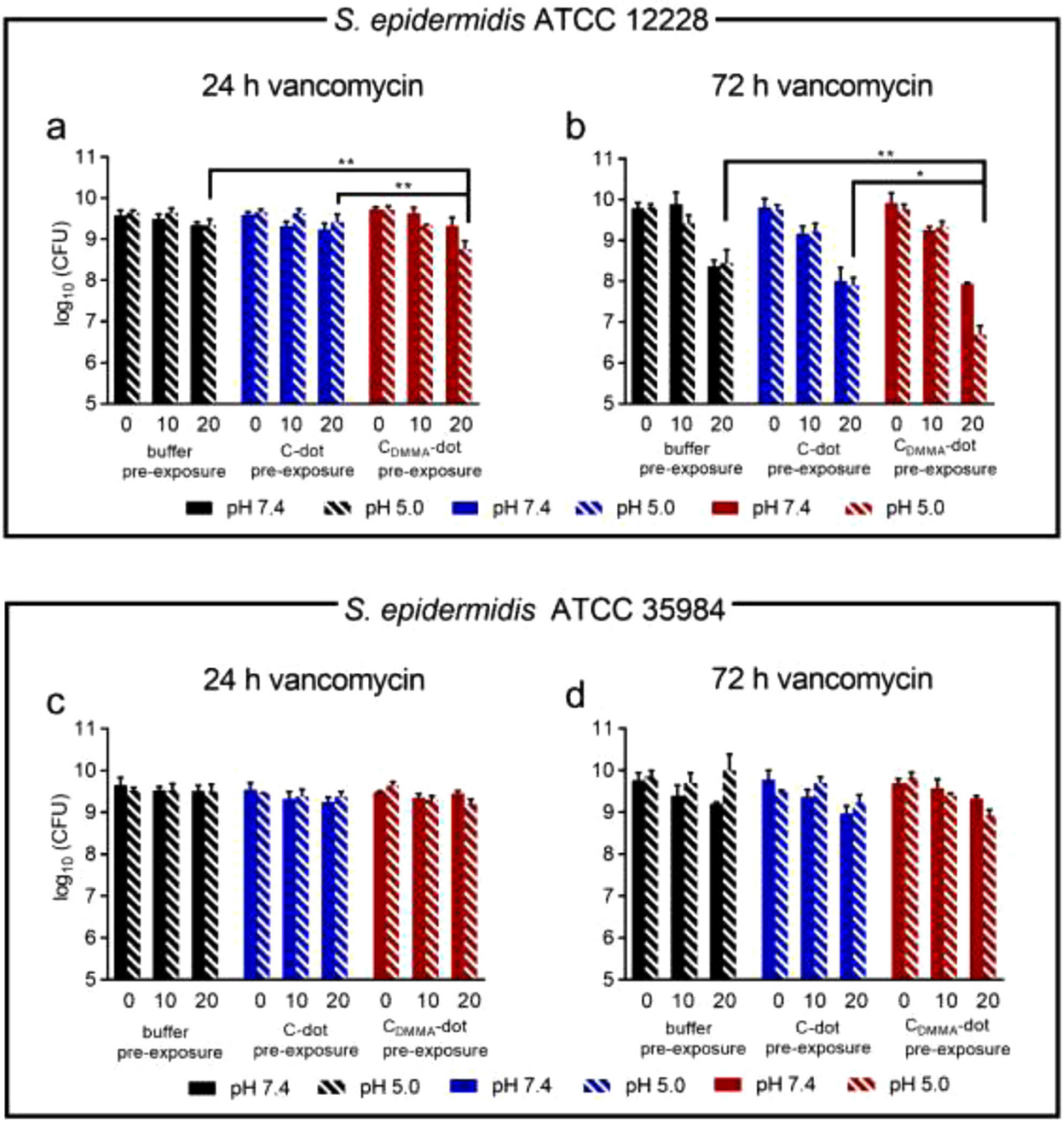

Fig. 6. Effects of pre-exposure of 24 h old staphylococcal biofilms to C- dots without DMMA or C_{DMMA}-dots (125 μg/mL) followed by subsequent growth in absence or presence of vancomycin (0 x, 10 x and 20 x the vancomycin MBC) on biofilm viability.
(a) Log_{10} CFU per biofilm of *S. epidermidis* ATCC 12228 biofilms after pre-exposure to buffer or carbon dot suspensions, followed by 24 h growth in presence of vancomycin for 24 h.
(b) Same as (a), but now for subsequent growth in presence of vancomycin for 72 h.
(c) Same as (a), but now for *S. epidermidis* ATCC 35984 biofilm.
(d) Same as (b), but now for *S. epidermidis* ATCC 35984 biofilm.
All data are expressed as means ± SD over triplicate experiments with separately prepared carbon dots and different staphylococcal cultures. *$p < 0.05$ and **$p < 0.01$ indicate significant differences with respect vancomycin in absence of prior carbon dot exposure or prior exposure to C-dots (one way ANOVA).

Carbon dots were imaged using Transmission Electron Microscopy (TEM). To this end, C-dots and C_{DMMA}-dots in demineralized water were put onto carbon coated copper grids and the excess solvent was allowed to evaporate. TEM images were taken using Philips CM 120 electron microscope operating at 120 kV (FEI, The Netherlands). In addition, diameters of the carbon dots were measured in 10 mM potassium phosphate buffer (100 μg carbon dots mL^{-1}) using Dynamic Light Scattering at 25 °C (Malvern Instruments, UK), while zeta potentials of the carbon dots were measured using the same instrument.

Presence of DMMA on the C_{DMMA}-dots was demonstrated using UV–vis absorption spectroscopy and NMR. ^1H NMR and ^{13}C NMR was carried out using D_2O water as a solvent (Bruker Avance 500 spectrometer, Germany). UV–vis absorption spectra were obtained in a quartz cuvette using UV–vis spectrophotometer (5082 PerkinElmer Lambda 2,

USA). Fluorescence emission spectra were measured using a Jasco spectrofluorometer FP-8300 (Japan). Carbon dots were suspended in 10 mM potassium phosphate buffer (pH 7.4 or pH 5.0) to an absorbance intensity below 0.1. The same suspensions were used to measure the quantum yield using quinine sulfate (0.1 M H_2SO_4; quantum yield 54%) as a standard [13].

The quantum yield of the carbon dots was calculated subsequently as

$$\Phi_x = \Phi_{st}\left(\frac{K_x}{K_{st}}\right)\left(\frac{\eta_x}{\eta_{st}}\right)^2 \quad (1)$$

in which Φ_x and Φ_{st} are the quantum yields of the nanoparticles to be determined and the standard applied, respectively, K_x and K_{st} are the slopes of a linear regression on the absorbance as a function of the integrated photoluminescence and η_x and η_{st} are the refractive indices of the nanoparticle suspension and the standard solution, respectively.

4.3. Staphylococcal growth conditions and harvesting

S. epidermidis ATCC 12228 and ATCC 35984 were grown on blood agar plates. Both strains had an MBC against vancomycin of 1.96 μg mL^{-1} as experimentally determined (see section *Minimal bactericidal concentration of C-dots without DMMA, C_{DMMA}-dots and DMMA in solution*) and in line with literature [50]. One colony was inoculated into Tryptone Soya Broth (10 mL, TSB, UK) and incubated under aerobic conditions for 24 h at 37 °C, subsequently inoculated in TSB (200 mL) and grown for 18 h. *S. epidermidis* cultures were harvested by centrifugation for 5 min at 5000*g* and washed twice with potassium phosphate buffer (10 mmol L^{-1}, pH 7.4). The bacterial suspension was sonicated for 3 × 10 s, while cooling in an ice/water bath to remove bacterial aggregates. Staphylococci were enumerated using a Bürker–Türk counting chamber and re-suspended in potassium phosphate buffer with the appropriate pH and bacterial concentration for the different experiments.

4.4. Carbon dot interaction with staphylococci

Zeta potential measurements were also applied to evaluate the interactions between staphylococci and carbon dots, as described before [51]. Briefly, staphylococcal suspensions (1×10^8 bacteria mL^{-1}) in potassium phosphate buffer (pH 7.4 and 5.0) were incubated with C-dots without DMMA or C_{DMMA}-dots (62.5, 125, 250, 500 μg mL^{-1}) for 30 min at 37 °C. After incubation, unbound carbon dots were removed by centrifugation (5000*g* for 10 min) and pellets of bacteria with attached carbon dots washed twice and re-suspended in potassium phosphate buffer (1 mL) for zeta potential measurements (Malvern Instruments, UK). Staphylococci were also incubated under the same conditions in buffer without carbon dots.

The driving forces involved in staphylococcal attachment to surfaces, including their partitioning in the predominantly aqueous biofilms leading to aggregate formation in a biofilm, were determined with a two phase partitioning assay, as previously described [38–41]. Briefly, staphylococcal suspensions (3 mL) in 10 mM potassium phosphate buffer at different pH values at an optical density at 600 nm between 0.4 and 0.6, were exposed to C-dots or C_{DMMA}-dots (500 μg mL^{-1}) for 30 min at 37 °C. After incubation, unbound carbon dots were removed by centrifugation (5000 *g* for 10 min) and pellets of bacteria with attached C-dots or C_{DMMA}-dots washed twice and re-suspended in 3 mL of potassium phosphate buffer with pH adjusted to different values between 5.0 and 7.4. The absorption at 600 nm was set as $[A_0]$. Hexadecane (1:20) was added to the bacterial suspension with and without the carbon dots and vortexed for 10 s. Finally, the suspension was allowed to settle for 10 min, and optical density was measured again (absorbance at time t $[A_t]$). This procedure was repeated for five more times to enable calculation of an initial removal rate from the aqueous phase defined as

$$\text{Rate of initial removal} = \lim_{t \to 0} \frac{d}{dt} \log\left(\frac{A_t}{A_0} x\ 100\right) \quad (2)$$

in which t is the vortexing time. The experiment was performed in triplicate with different bacterial cultures.

4.5. Minimal bactericidal concentration of C-dots without DMMA, C_{DMMA}-dots and DMMA in solution

To determine the MBC of C-dots without DMMA and C_{DMMA}-dots, *S. epidermidis* ATCC 12228 and ATCC 35984 (2×10^5 bacteria mL^{-1}) were suspended in 15% TSB (100 μL) at pH 7.4 or pH 5.0. C-dots without DMMA, C_{DMMA}-dots, or DMMA (initial concentration 1 mg mL^{-1}) were added in two-fold serial dilutions in a 96 well-plates and incubated for 24 h at 37 °C. Subsequently, the MBC values were determined by plating aliquots of the bacterial suspensions yielding no visible growth after 24 h on TSB agar plates. After 24 h incubation at 37 °C, the lowest concentration at which colony formation remained absent, was taken as the MBC.

The MBC of *S. epidermidis* ATCC 12228 and ATCC 35984 was determined against vancomycin as described above, but in 100% TSB.

4.6. Biofilm exposure to C-dots without DMMA, C_{DMMA}-dots and DMMA in solution

Bacterial suspension in potassium phosphate buffer at pH 7.4 (1 mL, 1×10^9 bacteria mL^{-1}) was added to a 12 well-plate and left for 2 h to allow staphylococcal adhesion at 37 °C. After 2 h, the bacterial suspension was removed and the well was washed once with phosphate buffer (pH 7.4). Two mL TSB was added to each well and bacteria were incubated at 37 °C. After 24 h, the TSB medium was removed and the *S. epidermidis* biofilms were washed once with potassium phosphate buffer at pH 7.4 or 5.0, depending on the experiment. Thus grown biofilms, were exposed to carbon dots suspensions (125 μg mL^{-1}) or DMMA alone (30 μg mL^{-1}) in potassium phosphate buffer pH 7.4 or pH 5.0 for 4 h, after which fluids were carefully removed, and biofilms washed twice with potassium phosphate buffer at the appropriate pH. Staphylococcal biofilms were also exposed to buffer, C-dots and C_{DMMA}-dots (125 μg mL^{-1}) at pH 5.0 for different time up to 4 h in order to study kinetic effects of exposure.

For CLSM (Leica TCS SP2 Leica, Germany), biofilms were immersed in LIVE/DEAD stain (*Bac*Light™, Molecular probes, The Netherlands) containing SYTO9 and propidium iodide for 20 min in the dark. After 20 min, the stain was removed and the biofilms were immersed in potassium phosphate buffer (pH 7.4 or pH 5.0) and imaged using CLSM. A solid state laser at 405 nm was used for excitation of the C-dots and C_{DMMA}-dots (blue fluorescent), an argon ion laser at 488 nm to excite SYTO9 (green fluorescent) and a HeNe laser at 543 nm was used to excite propidium iodide (red fluorescent), collecting fluorescences at 430 − 480 nm (C-dots/C_{DMMA}-dots), 500–535 nm (SYTO9) and 583–688 nm (propidium iodide). Biofilm images were further analyzed using ImageJ and COMSTAT to determine biofilm thickness and the percentage of live/dead bacteria [43]. After taking confocal images, biofilms were sonicated for 30 s and the total number of bacteria (live and dead) per biofilm derived using a Bürker–Türk counting chamber.

4.7. Combined effects of pre-exposure of biofilms to carbon dots followed by antibiotics

24 h staphylococcal biofilms were pre-exposed to C-dots without DMMA or C_{DMMA}-dots (125 μg/mL) in potassium phosphate buffer at pH 7.4 and pH 5.0 for 4 h. After 4 h, carbon dot suspensions were removed, biofilms washed twice with potassium phosphate buffer at the appropriate pH and vancomycin (10 and 20 times MBC) in TSB medium

was added for subsequent growth in presence of antibiotics for 24 or 72 h. For 72 h exposure, the vancomycin solution was refreshed every 24 h. After vancomycin exposure, biofilm bacteria were removed as described above (see section *Biofilm Exposure to C-dots without DMMA, CDMMA-dots and DMMA in solution*) and the number of CFUs per biofilm determined by serial dilutions and plated on the TSB agar plates. CFUs were counted after 24 h incubation.

4.8. Statistics analysis

The differences in biofilm properties were compared using one way ANOVA. Differences were considered significant if $p < 0.05$. Statistical analysis was performed using GraphPad version 7.00 (GraphPad Software, USA).

CRediT authorship contribution statement

Yanyan Wu: Conceptualization, Methodology, Validation, Formal analysis, Data curation, Investigation, Visualization, Writing - original draft. **Henny C. van der Mei:** Conceptualization, Methodology, Validation, Formal analysis, Visualization, Supervision, Writing - review & editing. **Henk J. Busscher:** Conceptualization, Methodology, Validation, Formal analysis, Resources, Visualization, Supervision, Writing - review & editing. **Yijin Ren:** Conceptualization, Validation, Formal analysis, Resources, Visualization, Supervision, Writing - review & editing, Funding acquisition.

Declaration of Competing Interest

HJB is also director of a consulting company SASA BV. Opinions and assertions contained herein are those of the authors and are not construed as necessarily representing views of the funding organization or their respective employer(s).

Acknowledgements

The project leading to this application has received funding from the European Union's Horizon 2020 research and innovation program under the MarieSkłodowska-Curie grant agreement No 713482.

Appendix A. Supplementary data

Supplementary material related to this article can be found, in the online version, at doi:https://doi.org/10.1016/j.colsurfb.2020.111114.

References

[1] D. Davies, Understanding biofilm resistance to antibacterial agents, Nat. Rev. Drug Discov. 2 (2003) 114–122.
[2] H.C. Flemming, J. Wingender, U. Szewzyk, P. Steinberg, S.A. Rice, S. Kjelleberg, Biofilms: an emergent form of bacterial life, Nat. Rev. Microbiol. 14 (2016) 563–575.
[3] T. Tolker-Nielsen, Biofilm development, Microbiol. Spectr. 3 (2) (2015) MB-0001-2014.
[4] H.C. Flemming, J. Wingender, The biofilm matrix, Nat. Rev. Microbiol. 8 (2010) 623–633.
[5] D. Fleming, K.P. Rumbaugh, Approaches to dispersing medical biofilms, Microorganisms 5 (2017) 15.
[6] X. Chen, X. Zhang, F. Lin, Y. Guo, F.-G. Wu, One-step synthesis of epoxy group-terminated organosilica nanodots: a versatile nanoplatform for imaging and eliminating multidrug-resistant bacteria and their biofilms, Small 15 (2019) 1901647.
[7] D.P. Gnanadhas, M. Elango, S. Janardhanraj, C.S. Srinandan, A. Datey, R.A. Strugnell, J. Gopalan, D. Chakravortty, Successful treatment of biofilm infections using shock waves combined with antibiotic therapy, Sci. Rep. 5 (2015) 17440.
[8] E. Teirlinck, R. Xiong, T. Brans, K. Forier, J. Fraire, H.V. Acker, N. Matthijs, R.D. Rycke, S.C.D. Smedt, T. Coenye, K. Braeckmans, Laser-induced vapour nanobubbles improve drug diffusion and efficiency in bacterial biofilms, Nat. Commun. 9 (2018) 4518.
[9] Y. Liu, L. Shi, L. Su, H.C. van der Mei, P.C. Jutte, Y. Ren, H.J. Busscher, Nanotechnology-based antimicrobials and delivery systems for biofilm-infection control, Chem. Soc. Rev. 48 (2019) 428–446.
[10] H.J. Busscher, V. Alt, H.C. van der Mei, P.H. Fagette, W. Zimmerli, T.F. Moriarty, J. Parvizi, G. Schmidmaier, M.J. Raschke, T. Gehrke, R. Bayston, L.M. Baddour, L.C. Winterton, R.O. Darouiche, D.W. Grainger, A trans-atlantic perspective on stagnation in clinical translation of antimicrobial strategies for the control of biomaterial-implant-associated infection, ACS Biomater. Sci. Eng. 5 (2019) 402–406.
[11] S. Zhu, Q. Meng, L. Wang, J. Zhang, Y. Song, H. Jin, K. Zhang, H. Sun, H. Wang, B. Yang, Highly photoluminescent carbon dots for multicolor patterning, sensors, and bioimaging, Angew. Chem. Int. Ed. 52 (2013) 3953–3955.
[12] S.K. Bhunia, A. Saha, A.R. Maity, S.C. Ray, N.R. Jana, Carbon nanoparticle-based fluorescent bioimaging probes, Sci. Rep. 3 (2013) 1473.
[13] C. Liu, P. Zhang, X. Zhai, F. Tian, W. Li, J. Yang, Y. Liu, H. Wang, W. Wang, W. Liu, Nano-carrier for gene delivery and bioimaging based on carbon dots with PEI-passivation enhanced fluorescence, Biomaterials 33 (2012) 3604–3613.
[14] T. Feng, X. Ai, G. An, P. Yang, Y. Zhao, Charge-convertible carbon dots for imaging-guided drug delivery with enhanced *in vivo* cancer therapeutic efficiency, ACS Nano 10 (2016) 4410–4420.
[15] J. Li, S. Yang, Y. Deng, P. Chai, Y. Yang, X. He, X. Xie, Z. Kang, G. Ding, H. Zhou, X. Fan, Emancipating target-functionalized carbon dots from autophagy vesicles for a novel visualized tumor therapy, Adv. Funct. Mater. 28 (2018) 1800881.
[16] J. Hou, Z. Tian, H. Xie, Q. Tian, S. Ai, A fluorescence resonance energy transfer sensor based on quaternized carbon dots and Ellman's test for ultrasensitive detection of dichlorvos, Sens. Actuators B Chem. 232 (2016) 477–483.
[17] J. Kim, J. Park, H. Kim, K. Singha, W.J. Kim, Transfection and intracellular trafficking properties of carbon dot-gold nanoparticle molecular assembly conjugated with PEI-pDNA, Biomaterials 34 (2013) 7168–7180.
[18] C. Wang, Z. Xu, C. Zhang, Polyethyleneimine-functionalized fluorescent carbon dots: water stability, pH sensing, and cellular imaging, ChemNanoMat 1 (2015) 122–127.
[19] W. Bing, H. Sun, Z. Yan, J. Ren, X. Qu, Programmed bacteria death induced by carbon dots with different surface charge, Small 12 (2016) 4713–4718.
[20] J.S. Sidhu, Mayank, T. Pandiyan, Navneet Kaur, N. Singh, The photochemical degradation of bacterial cell wall using penicillin-based carbon dots: weapons against multi-drug resistant (MDR) strains, ChemistrySelect 2 (2017) 9277–9283.
[21] H. Sun, N. Gao, K. Dong, J. Ren, X. Qu, Graphene quantum dots-band-aids used for wound disinfection, ACS Nano 8 (6) (2014) 6202–6210.
[22] F. Lin, C. Li, Z. Chen, Bacteria-derived carbon dots inhibit biofilm formation of *Escherichia coli* without affecting cell growth, Front. Microbiol. 9 (2018) 259.
[23] Y.-J. Li, S.G. Harroun, Y.-C. Su, C.-F. Huang, B. Unnikrishnan, H.-J. Lin, C.-H. Lin, C.-C. Huang, Synthesis of self-assembled spermidine-carbon quantum dots effective against multidrug-resistant bacteria, Adv. Healthcare Mater. 5 (2016) 2545–2554.
[24] H.-H. Ran, X. Cheng, Y.-W. Bao, X.-W. Hua, G. Gao, X. Zhang, Y.-W. Jiang, Y.-X. Zhu, F.-G. Wu, Multifunctional quaternized carbon dots with enhanced biofilm penetration and eradication efficiencies, J. Mater. Chem. B Mater. Biol. Med. 7 (2019) 5104–5114.
[25] F. Lin, C. Li, L. Dong, D. Fua, Z. Chen, Imaging biofilm-encased microorganisms using carbon dots derived from *L. Plantarum*, Nanoscale 9 (2017) 9056–9064.
[26] C. Zhu, H. Li, H. Wang, B. Yao, H. Huang, Y. Liu, Z. Kang, Negatively charged carbon nanodots with bacteria resistance ability for high-performance antibiofilm formation and anticorrosion coating design, Small 15 (2019) 1900007.
[27] X.W. Hua, Y.W. Bao, H.Y. Wang, Z. Chen, F.G. Wu, Bacteria-derived fluorescent carbon dots for microbial live/dead differentiation, Nanoscale 9 (2017) 2150–2161.
[28] J. Yang, X. Zhang, Y.H. Ma, G. Gao, X. Chen, H.R. Jia, Y.H. Li, Z. Chen, F.G. Wu, Carbon dot-based platform for simultaneous bacterial distinguishment and antibacterial applications, ACS Appl. Mater. Interfaces 8 (2016) 32170–32181.
[29] W. Ziebuhr, S. Hennig, M. Eckart, H. Kranzler, C. Batzilla, S. Kozitskaya, Nosocomial infections by *Staphylococcus epidermidis*: how a commensal bacterium turns into a pathogen, J. Antimicrob. Agents 28S (2006) S14–S20.
[30] K.O. Oduwole, A.A. Glynn, D.C. Molony, D. Murray, S. Rowe, L.M. Holland, D.J. McCormack, J.P. O'Gara, Anti-biofilm activity of sub-inhibitory povidone-iodine concentrations against *Staphylococcus epidermidis* and *Staphylococcus aureus*, J. Orthop. Res. 28 (2010) 1252–1256.
[31] A.L.J. Olsson, H.C. van der Mei, H.J. Busscher, P.K. Sharma, Acoustic sensing of the bacterium–substratum interface using QCM-D and the influence of extracellular polymeric substances, J. Colloids Interface Sci. 357 (2011) 135–138.
[32] C.R. Arciola, D. Campoccia, L. Baldassarri, M.E. Donati, V. Pirini, S. Gamberini, L. Montanaro, Detection of biofilm formation in *Staphylococcus epidermidis* from implant infections. Comparison of a PCR-method that recognizes the presence of ica genes with two classic phenotypic methods, J. Biomed. Mater. Res. A. 2 (76A) (2006) 425–430.
[33] C.R. Arciola, L. Baldassarri, L. Montanaro, Presence of icaA and icaD genes and slime production in a collection of staphylococcal strains from catheter-associated infections, J. Clin. Microbiol. 39 (2001) 2151–2156.
[34] S. Nandi, M. Ritenberg, R. Jelinek, Bacterial detection with amphiphilic carbon dots, Analyst 140 (2015) 4232–4237.
[35] J.H. Lee, Y. Gu, H. Wang, W.Y. Lee, Microfluidic 3D bone tissue model for high-throughput evaluation of wound-healing and infection-preventing biomaterials, Biomaterials 33 (2012) 999–1006.
[36] J. Xiao, A.T. Hara, D. Kim, D.T. Zero, H. Koo, G. Hwang, Biofilm three-dimensional architecture influences in situ pH distribution pattern on the human enamel surface, Int. J. Oral Sci. 9 (2017) 74–79.
[37] R. Bos, H.J. Busscher, Role of acid–base interactions on the adhesion of oral streptococci and actinomyces to hexadecane and chloroform—influence of divalent cations and comparison between free energies of partitioning and free energies obtained by extended DLVO analysis, Colloids Surf. B Biointerfaces 14 (1999) 169–177.

[38] M. Rosenberg, D. Gutnick, E. Rosenberg, Adherence of bacteria to hydrocarbons: a simple method for measuring cell-surface hydrophobicity, FEMS Microbiol. Lett. 9 (1980) 29–33.
[39] D. Lichtenberg, M. Rosenberg, N. Sharfman, I. Ofek, A kinetic approach to bacterial adherence to hydrocarbon, J. Microbiol. Methods 4 (1985) 141–146.
[40] H.J. Busscher, B. van de Belt-Gritter, H.C. van der Mei, Implications of microbial adhesion to hydrocarbons for evaluating cell surface hydrophobicity 1. Zeta potentials of hydrocarbon droplets, Colloids Surf. B Biointerfaces 5 (1995) 111–116.
[41] H.C. van der Mei, B. van der Belt-Gritter, H.J. Busscher, Implications of microbial adhesion to hydrocarbons for evaluating cell surface hydrophobicity 2. Adhesion mechanisms, Colloids Surf. B Biointerfaces 5 (1995) 117–126.
[42] B.W. Peterson, Y. He, Y. Ren, A. Zerdoum, M.R. Libera, P.K. Sharma, A.-J. van Winkelhoff, D. Neut, P. Stoodley, H.C. van der Mei, H.J. Busscher, Viscoelasticity of biofilms and their recalcitrance to mechanical and chemical challenges, FEMS Microbiol. Rev. 39 (2015) 234–245.
[43] A. Heydorn, A.T. Nielsen, M. Hentzer, C. Sternberg, M. Givskov, B.K. Ersbøll, S. Molin, Quantification of biofilm structures by the novel computer program COMSTAT, Microbiology 146 (2000) 2395–2407.
[44] J.L. Lister, A.R. Horswill, *Staphylococcus aureus* biofilms: recent developments in biofilm dispersal, Front. Cell. Infect. Microbiol. 4 (2014) 178.
[45] Z. Chen, H. Ji, C. Liu, W. Bing, Z. Wang, X. Qu, A multinuclear metal complex based DNase-mimetic artificial enzyme: matrix cleavage for combating bacterial biofilms, Angew. Chem. 128 (2016) 10890–10894.
[46] H.-J. Jian, R.-S. Wu, T.Y. Lin, Y.-J. Li, H.-J. Lin, S.G. Harroun, J.-Y. Lai, C.-C. Huang, Super-cationic carbon quantum dots synthesized from spermidine as an eye drop formulation for topical treatment of bacterial keratitis, ACS Nano 11 (2017) 6703–6716.
[47] L. Hui, J. Huang, G. Chen, Y. Zhu, L. Yang, Antibacterial property of graphene quantum dots (both source material and bacterial shape matter), ACS Appl. Mater. Interfaces 8 (2016) 20–25.
[48] X. Zhang, X. Chen, J. Yang, H.R. Jia, Y.H. Li, Z. Chen, F.G. Wu, Quaternized silicon nanoparticles with polarity-sensitive fluorescence for selectively imaging and killing gram-positive bacteria, Adv. Funct. Mater. 26 (2016) 5958–5970.
[49] S. Huo, Y. Jiang, A. Gupta, Z. Jiang, R.F. Landis, S. Hou, X.-J. Liang, V.M. Rotello, Fully zwitterionic nanoparticle antimicrobial agents through tuning of core size and ligand structure, ACS Nano 10 (2016) 8732–8737.
[50] K.L. LaPlante, L.A. Mermel, In vitro activity of daptomycin and vancomycin lock solutions on staphylococcal biofilms in a central venous catheter model, Nephrol. Dial. Transplant. 22 (8) (2007) 2239–2246.
[51] J. Li, K. Zhang, L. Ruan, S.F. Chin, N. Wickramasinghe, H. Liu, V. Ravikumar, J. Ren, H. Duan, L. Yang, M.B. Chan-Park, Block copolymer nanoparticles remove biofilms of drug-resistant gram-positive bacteria by nanoscale bacterial debridement, Nano Lett. 18 (2018) 4180–4187.